

Effect of pressure on the Raman scattering of wurtzite AlN

F. J. Manjón^{*,1,2}, D. Errandonea¹, N. Garro¹, A. H. Romero³, J. Serrano⁴, and M. Kuball⁵

¹ Dpto. de Física Aplicada-ICMUV, Univ. de València, c/Dr. Moliner 50, 46100 Burjassot, Spain

² Dpto. de Física Aplicada, Univ. Politècnica de València, Cno. de Vera s/n, 46022 València, Spain

³ CINVESTAV, 76230 Querétaro, México

⁴ European Synchrotron Radiation Facility, BP 220, 38043 Grenoble Cedex, France

⁵ H. H. Wills Physic Laboratory, University of Bristol, Bristol BS8 1TL, United Kingdom

Received 23 June 2006, revised 25 August 2006, accepted 27 August 2006

Published online 27 November 2006

PACS 61.50.Ks, 62.50.+p, 63.20.Dj, 78.30.Fs

High-pressure Raman spectra of wurtzite aluminum nitride were measured up to 25 GPa. The Raman-active modes in wurtzite-AlN were obtained up to the wurtzite-to-rocksalt transition at 20 GPa and their pressure coefficients compared with those obtained from *ab initio* lattice dynamics calculations. A slight decrease of the LO–TO splitting under pressure has been measured. We also report Raman scattering of the rocksalt phase of AlN during downstroke. The comparison of previously reported Raman scattering in rocksalt-GaN and *ab initio* calculations suggests that the Raman scattering we have measured in rocksalt-AlN likely corresponds to the one-phonon density of states of the rocksalt phase. A partial return to the wurtzite phase is found at ambient pressure after fully releasing pressure.

© 2007 WILEY-VCH Verlag GmbH & Co. KGaA, Weinheim

1 Introduction

The interest in the study of the vibrational properties of AlN under compression has increased in the last years. Perlin et al. performed the first high-pressure Raman studies, estimating the pressure coefficients of three of the six Raman-active modes [1]. Kuball et al. carried out similar measurements, determining the pressure coefficients of five modes. They reported that under pressure the LO–TO (E_1) splitting slightly decreases and the LO–TO (A_1) splitting increases [2]. Afterwards, Goñi et al. compared the pressure dependence of the Raman-active modes in GaN and AlN with *ab initio* calculations and found a small but increasing LO–TO (E_1) splitting under pressure [3]. However, a decrease of the LO–TO splitting for both A_1 and E_1 modes was estimated in recent Raman measurements of Yakovenko et al. [4]. To our knowledge, this work is the only one reporting the pressure dependence of the six Raman-active modes of wurtzite (wz) AlN up to the wurtzite-to-rocksalt phase transition. However, regarding the vibrational properties of AlN with decreasing pressure after this transition occurred there is no information available yet. In this work we report on the pressure dependence of the six Raman-active modes of wz-AlN up to the phase transition near 20 GPa and compare them with our *ab initio* lattice dynamics calculations. We also analyze the behaviour of the vibrational properties of AlN with decreasing pressure following the high-pressure phase transition and comparing it with that reported previously in GaN.

* Corresponding author: e-mail: fmanjon@fis.upv.es

2 Experimental details

A single crystal of wz-AlN ($100 \times 100 \mu\text{m}$ and $30 \mu\text{m}$ thick) was loaded in a diamond anvil cell (DAC) using a 4:1 methanol–ethanol mixture as pressure-transmitting medium. The pressure was determined using a ruby chip as pressure sensor [5]. Raman experiments at room temperature (RT) were performed in backscattering geometry using the 514.5 nm line of an Ar^+ laser and a Jobin–Yvon T64000 triple spectrometer in combination with a multi-channel CCD detector. Spectral resolution was around 1 cm^{-1} . Argon and Neon plasma lines were used to calibrate the spectra.

3 Calculation details

Theoretical calculations were performed in the framework of the local-density approximation (LDA) of the density functional theory (DFT) as implemented in the ABINIT package [6]. The Kohn–Sham orbitals were expanded in plane waves up to a cutoff of 70 Ry for wz-AlN and rocksalt-GaN (rs-GaN) after explicitly checking energy convergence up to 0.0001 eV/atom. Pseudopotentials were generated using the Troullier–Martins scheme [7] (3s and 3p electrons were considered for Al, 2s and 2p for N, and 4s and 4p for Ga). Non-linear core corrections were included for Ga atoms [8]. Integrals over the Brillouin zone were replaced by a sum on meshes of $8 \times 8 \times 4$ for the wz and $5 \times 5 \times 5$ for the rs structures.

The lattice dynamics were calculated after relaxation of the lattice parameters to the minimal energy structure as function of pressure. The dynamical matrix, vibrational dispersion curves and vibrational density of states were computed within the linear response formalism of density functional perturbation theory [9]. The dynamical matrices were calculated for a mesh of q-points ($6 \times 6 \times 3$ for wz and $4 \times 4 \times 4$ for rs) in the irreducible Brillouin zone and then interpolated to obtain the phonon dispersion [9].

4 Results and discussion

Figure 1 presents the Raman spectra of AlN at different pressures during the upstroke showing the six Raman-active modes of the wz structure. The $A_1(\text{LO})$, $E_2(\text{low})$, and $E_1(\text{LO})$ can be tracked up to 9 GPa, 12 GPa, and 14 GPa, respectively. The other three Raman peaks of the wz phase vanish above 18 GPa.

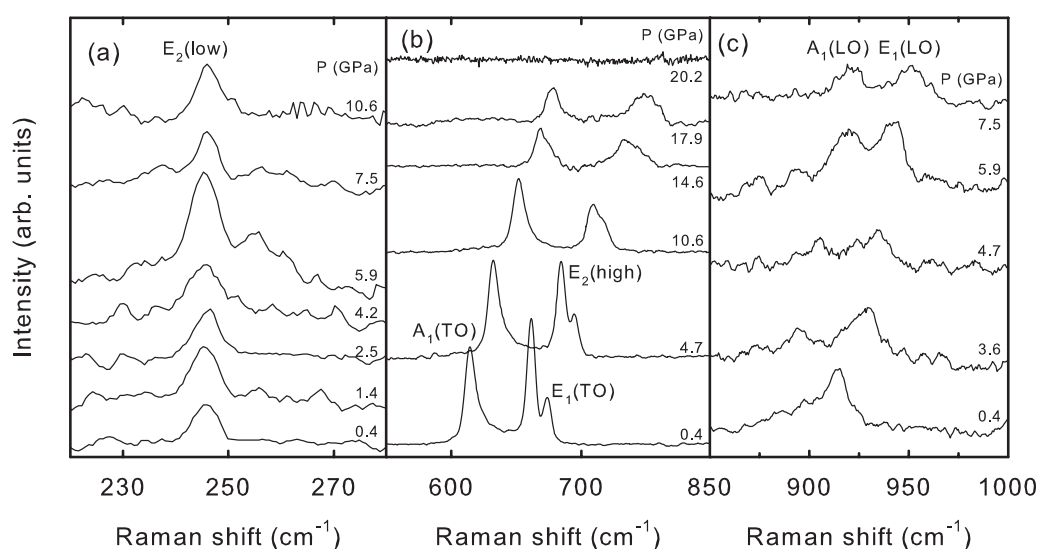


Fig. 1 RT Raman spectra of wurtzite AlN in the low-frequency region up to 11 GPa (a), in the middle-frequency region up to 20 GPa (b), and in the high-frequency region up to 8 GPa (c).

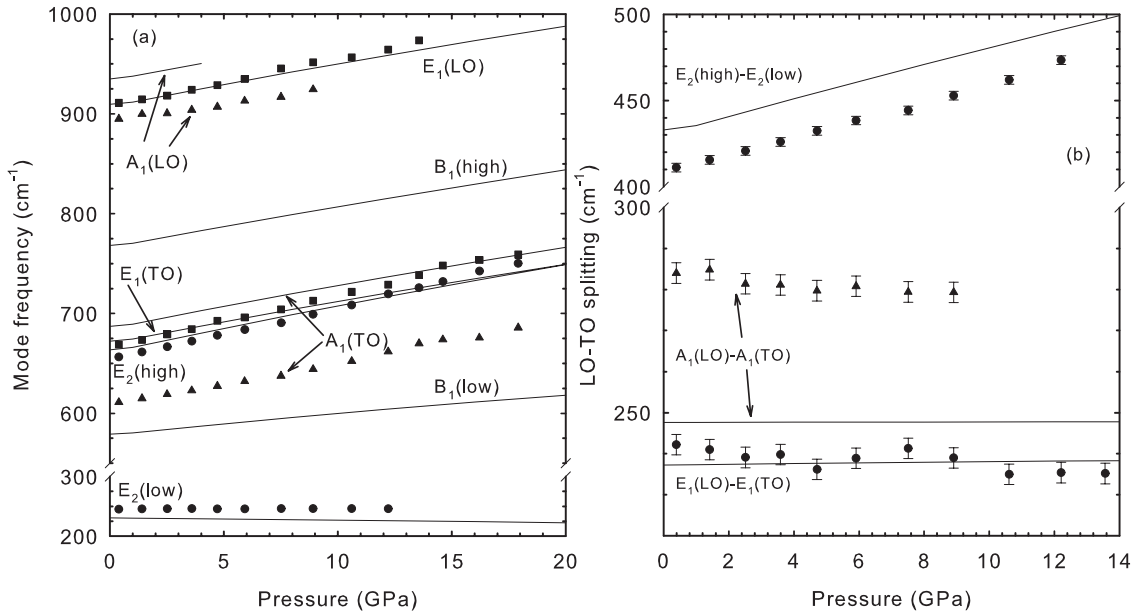


Fig. 2 Pressure dependence of the experimental (symbols) and calculated (lines) vibrational modes of the wurtzite phase of AlN (a), and of the $E_2(\text{high})-E_2(\text{low})$ and LO-TO (A_1 and E_1) splitting (b).

The pressure dependence of the measured modes compared with that obtained from our *ab initio* calculations is depicted in Fig. 2(a).

Table 1 summarizes our measured and calculated Raman frequencies and pressure coefficients at zero pressure where they are compared to values reported in the literature. The frequencies (pressure coefficients) obtained from our calculations for the silent $B_1(\text{low})$ and $B_1(\text{high})$ modes are 579 cm^{-1} ($2.08 \text{ cm}^{-1}/\text{GPa}$) and 767 cm^{-1} ($3.77 \text{ cm}^{-1}/\text{GPa}$), respectively, in good agreement with the values of 580.7 and 781.6 cm^{-1} reported by inelastic X-ray measurements [10]. It is noteworthy the good agreement between the experimental and calculated frequencies for the E_2 and E_1 modes. However, there is a poor agreement for the A_1 mode frequencies, despite the good agreement in the pressure coefficients. We do not know at present the cause for this disagreement.

Table 1 Zero-pressure frequencies (ω_0 in cm^{-1}) and pressure coefficients ($d\omega_0/dP$ in $\text{cm}^{-1}/\text{GPa}$) of the Raman-active modes of wz-AlN. Experimental (Exp.) and theoretical (The) results are compared.

$E_2(\text{low})$		$A_1(\text{TO})$		$E_2(\text{high})$		$E_1(\text{TO})$		$A_1(\text{LO})$		$E_1(\text{LO})$		Ref.
ω_0	$d\omega_0/dP$	ω_0	$d\omega_0/dP$	ω_0	$d\omega_0/dP$	ω_0	$d\omega_0/dP$	ω_0	$d\omega_0/dP$	ω_0	$d\omega_0/dP$	
246(2)	0.07(1)	608(1)	4.35(3)	653(1)	5.40(4)	666(1)	5.33(4)	893(2)	3.70(2)	908(2)	4.77(3)	Exp ^a
		610	4.08	656	5.39	669	5.07	890	4.00	911	5.51	Exp ^b
247.5	0.12	608.5	4.40	655.5	4.99	669.3	4.55	891		910.1	4.60	Exp ^c
249	0.05	610	4.05	657	4.78	669	4.52	890	4.00	910	3.60	Exp ^d
241		607	4.63	660	3.99					924	1.67	Exp ^e
231	-0.33	686	4.01	663	4.34	672	3.90	934	4.03	909	3.99	The ^a
241	-0.03	618	3.00	667	3.80	677	3.80	898	3.50	924	4.00	The ^c
236	-0.29	628	4.29	631	4.79	649	4.36					The ^f

^a This work, ^b Ref. [2], ^c Refs. [3, 11], ^d Ref. [4], ^e Ref. [1], ^f Ref. [13].

Also interesting is the difference between the pressure coefficient found experimentally and theoretically for the $E_2(\text{low})$ mode. Experiments show a small but positive pressure coefficient while *ab initio* calculations give a small but negative one (see Table 1). The agreement of all experimental measurements in the pressure coefficient of the $E_2(\text{low})$ mode points towards a limitation of the *ab initio* calculations probably related to an inaccurate description of the long-range force constants. The latter would be improved by using a larger mesh of q -points prior to the interpolation of the dynamical matrices.

Figure 2(b) shows the pressure dependence of the LO–TO splittings in the wz phase. According to our measurements both the LO–TO splitting of both the A_1 and E_1 modes are almost constant or even decrease slightly with increasing pressure as already found by Yakovenko et al. [4]. This behavior is in reasonable agreement with our *ab initio* calculations, which yield an almost constant LO–TO splitting for both modes with pressure. On the other hand, an increase of the LO–TO splitting for the A_1 mode was found by Kuball et al. [2] and Goñi et al. [3] and attributed to the decrease of the refractive index with pressure in AlN as suggested by *ab initio* calculations [11]. *Ab initio* calculations of Wagner et al. also reported an increase of both LO–TO splittings of the A_1 and E_1 modes with increasing pressure [3, 11].

The experimental discrepancies could be due to differences in sample preparation and pressure environment that may affect the pressure response of the Raman modes in AlN [4]. Additionally, the weak intensity of the TO and LO modes reported in Ref. [2] might have resulted in an inaccurate determination of the pressure coefficients and LO–TO splittings. No high-pressure Raman spectra are shown in Ref. [3], preventing the direct comparison between those results and ours. The fact that only Yakovenko et al. [4] and us reported Raman spectra where the six modes of wz -AlN are observed up to at least 9 GPa, and the agreement between both results make us confident on the accuracy of our experiments. The constant or even decreasing LO–TO splittings under pressure measured and calculated by us in AlN are a consequence of the larger covalent character of the Al–N bond as compared to GaN. Our results for AlN agree with the general decrease of the LO–TO splittings caused by pressure for most covalent III–V and II–VI semiconductors [12].

Figure 3 shows the Raman spectra of AlN on pressure release from 25 GPa down to 1 atm. The spectra are dominated by several peaks (depicted by arrows) which do not move with pressure and which we

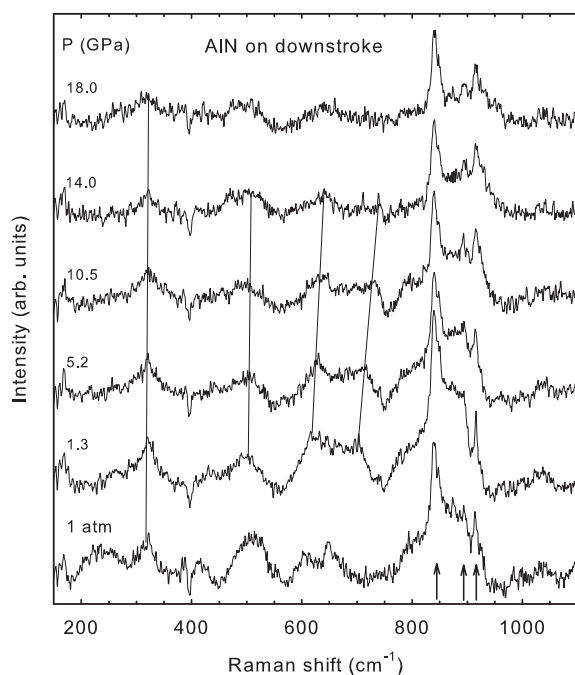


Fig. 3 RT Raman spectra of AlN on decreasing pressure from 25 GPa to 1 atm. Lines are guides to the eye showing the pressure behaviour of selected modes. Arrows show the position of peaks assigned to the methanol–ethanol mixture.

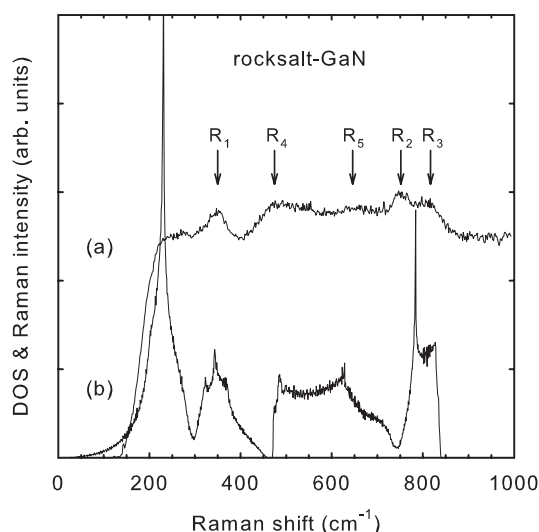


Fig. 4 (a) *Ab initio* calculated one-phonon density of states of rs-GaN at 50 GPa. (b) Experimental spectrum of GaN at 51 GPa after Ref. [14].

therefore attribute to the solidification of the methanol–ethanol mixture. Below 14 GPa there is a progressive increase of the overall Raman scattering intensity and several features, whose pressure dependence has been indicated with lines in Fig. 3, can be distinguished. The clearest features are: the appearance of a broad band whose intensity increases with decreasing pressure coincident in frequency with the peaks attributed to the methanol–ethanol mixture, and the progressive frequency shift of a broad band centred around 650 cm^{-1} at 1.3 GPa with two marked maxima. The increase of the Raman scattering of this band reaches its maximum at 1.3 GPa. However, the Raman spectrum at ambient pressure after fully releasing the pressure looks rather different to that at 1.3 GPa thus suggesting: 1) that a phase transition is taking place below 1 GPa; and 2) that the Raman spectra of AlN on downstroke from 25 to 1.3 GPa could correspond to the rs phase of AlN.

Raman scattering of the rs phase was observed in GaN above 46 GPa [14] and in InN above 15 GPa [15]. Therefore, a better understanding of the Raman scattering in these compounds could help us in the understanding of rs-AlN. To this aim we show in Fig. 4 the Raman spectrum of GaN at 51 GPa and our calculated one-phonon density of states (DOS) for rs-GaN at 50 GPa. The agreement between the experimental spectrum and calculations is good. In fact, from our calculations we can attribute the different features in the Raman spectrum of GaN at 51 GPa to: the LA(X) branch (R_1), the LO(X) branch (R_2), the LO(L) branch (R_3), the TO(Γ -L) branch (R_4), and the TO(X) branch (R_5). The observation of Raman scattering from rs-InN and rs-GaN and this agreement between the calculated one-phonon DOS and the experimental spectrum in rs-GaN could suggest that the Raman scattering observed in rs-InN and -AlN in the downstroke between 25 and 1.3 GPa and shown in Fig. 3 could likely correspond to the one-phonon DOS of the rs phase. *Ab initio* lattice dynamics calculations of the one- and two-phonon DOS in rs-AlN are under way and will be reported in a forthcoming paper to validate the above hypothesis.

5 Conclusions

The Raman scattering of wz-AlN has been measured up to 25 GPa. The pressure dependence of the wz Raman modes in AlN has been measured and calculated up to the wz-to-rs phase transition near 20 GPa. An experimental decrease of the LO–TO (A_1 and E_1) splitting has been found. On decrease of pressure from 25 GPa, we have measured Raman scattering in the rs phase that likely corresponds to the one-phonon density of states. A partial return of the sample to the wz phase is observed after fully release of pressure.

Acknowledgments This study was supported by the Spanish MCYT under grant MAT2002-04539-CO2-02. The authors thank A. Cantarero for providing access to the experimental Raman setup. F.J.M. thanks the financial support from the “Programa de Incentivo a la Investigación” of the Universidad Politécnica de Valencia. D.E. and N.G. acknowledge the financial support from the MEC of Spain through the “Ramón y Cajal” program. A.H.R. is supported by the project J-42647-F from CONACYT-Mexico.

References

- [1] P. Perlin, A. Polian, and T. Suski, *Phys. Rev. B* **47**, 2874 (1993).
- [2] M. Kuball, J. M. Hayes, A. D. Prins et al., *Appl. Phys. Lett.* **78**, 724 (2001).
M. Kuball, J. M. Hayes, Y. Shi et al., *J. Cryst. Growth* **231**, 391 (2001).
- [3] A. R. Goñi, H. Siegle, K. Syassen, C. Thomsen, and J. M. Wagner, *Phys. Rev. B* **64**, 035205 (2001).
- [4] E. V. Yakovenko, M. Gauthier, and A. Polian, *JETP* **98**, 981 (2004).
- [5] G. J. Piermarini, S. Block, J. D. Barnett, and R. A. Forman, *J. Appl. Phys.* **46**, 2774 (1975).
- [6] X. Gonze, J.-M. Beuken, R. Caracas, F. Detraux, M. Fuchs, G.-M. Rignanese, L. Sindic, M. Verstraete, G. Zerah, F. Jollet, M. Torrent, A. Roy, M. Mikami, Ph. Ghosez, J.-Y. Raty, and D. C. Allan, *Comput. Mater. Sci.* **25**, 478–492 (2002).
- [7] N. Trouiller and J. L. Martins, *Phys. Rev. B* **43**, 1993 (1991).
- [8] S. G. Louie, S. Froyen, and M. L. Cohen, *Phys. Rev. B* **26**, 1738 (1982).
- [9] S. Baroni, P. Gianozzi, and A. Testa, *Phys. Rev. Lett.* **58**, 1861 (1987).
- [10] M. Schwoerer-Böhning and A. T. Macrander, *J. Phys. Chem. Solids* **61**, 485 (2000).
- [11] J.-M. Wagner and F. Bechstedt, *Phys. Rev. B* **62**, 4526 (2000).
- [12] M. D. Frogley, D. J. Dunstan, and W. Palos, *Solid State Commun.* **107**, 537 (1998).
- [13] I. Gorczyca, N. E. Christensen, E. L. Peltzer y Blancá, and C. O. Rodríguez, *Phys. Rev. B* **51**, 11936 (1995).
- [14] M. P. Halsall, P. Harmer, P. J. Parbrook, and S. J. Henley, *Phys. Rev. B* **69**, 235207 (2004).
- [15] C. Pinquier, F. Demangeot, J. Frandon, J.-C. Chervin, A. Polian, B. Couzinet, P. Munsch, O. Briot, S. Ruffenach, B. Gil, and B. Maleyre, *Phys. Rev. B* **73**, 115211 (2006).